Regenerative Braking Control of the Brushless DC Motor Drive

Greg Emmen
ECE 517 – Fall 2021

***Abstract* – Brushless DC motors are commonly found in automotive applications. These motors require a controlled three-phase current to operate under standard conditions. This control is commonly implemented by use of a six-switch inverter. It is also desirable to include regenerative braking as a feature for battery and hybrid electric vehicles, requiring additional controls and hardware for implementation. This project introduces a modified six-switch inverter strategy for providing brake torque and regenerative capability. It also details the supporting hardware and controls necessary to implement the modified six-switch inverter strategy into a battery electric vehicle architecture.**

***Index Terms* – Battery Electric Vehicle (BEV), Bi-Directional DC/DC Converter, Brushless DC Motor (BLDC), HV Battery Charging, Hysteresis Control, Six-Switch Inverter, Regenerative Braking**

I. Introduction

A. Overview

As more hybrid and battery electric vehicles reach the market, different technologies are being explored to improve energy efficiency and vehicle range.

Regenerative braking is a common feature found on battery and hybrid electric vehicles. The idea of regenerative braking is that the existing system (motor/battery/inverter) works in tandem with the propulsion system to translate available kinetic energy into electrical energy that can be stored for later use [1]. This is completed in a method that has the additional purpose of decreasing vehicle speed without the need for application of friction brakes.

The methods for achieving a charge-capable voltage from the motor via regenerative braking can vary between systems depending on the hardware available. This project details the implementation of a control strategy and the supporting power electronics to utilize the trapezoidal back-emf of a BLDC motor for regenerative braking.

B. BLDC Motors

BLDC motors are a popular choice in the automotive industry for several reasons, as listed below:

1. Benefits
    a. Longer component life and less maintenance

Primarily due to the lack of commutation brushes, reducing the need for a high-wear component that requires replacement on occasion. This can make BLDC motors desirable for operating in locations where regular maintenance can be difficult or costly [2].

    b. High efficiency

Without the commutation brushes introducing friction during standard operation, BLDC motors see can see much higher efficiencies than other motor designs given the correct operating conditions [2]. This is important for the automotive industry where battery electric vehicle range is a critical design factor.

2. Drawbacks
    a. Requires complex control

BLDC motors operate by the application of a controlled three-phase current. This adds the requirement for a DC/AC inverter that is controlled using feedback from additional sensors. The implementation of a control system to manage a BLDC motor can be costly when compared to their brushed DC counterparts [3].

    b. Back-emf generation is unavoidable

In accordance with Faraday's law, the stator windings (a charge carrying conductor) are within a changing magnetic field (the spinning permanent magnet rotor) under standard operation; generating an electromotive force that opposes the current flow of the motor [4].

For BLDC motors the back-emf takes an ideal trapezoidal form as seen in Figure 1.

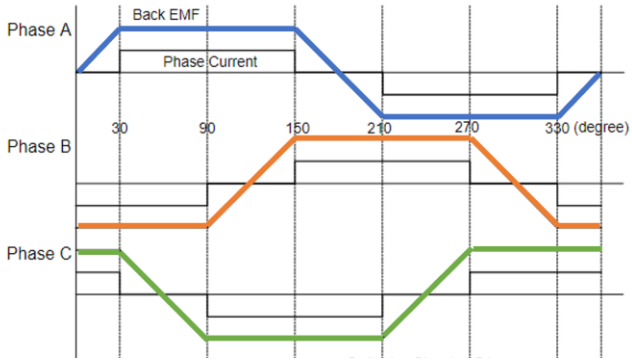

Figure 1: Ideal trapezoidal back-emf

Equations governing the back-emf generation are as follows:

$$EMF = \left(2N_s B_f l r\right) \cdot \omega = k_e \cdot \omega \quad (1)$$

Where:

- ω is the mechanical rotational speed
- k_e is the back-emf constant

This equation only holds true when the back-emf is constant. Lenz's law dictates that the back-emf is directly proportional to the speed of the rotor and can be calculated using the changing permanent magnet flux of the motor [5]. A more accurate differential equation to depict back-emf is as follows:

$$EMF = \frac{d\Phi}{dt} = \frac{\partial \Phi}{\partial \theta}\omega \quad (2)$$

Where:

- Φ is the permanent magnet flux linkage
- θ is the rotor angle

C. *Regenerative Braking*

The two main goals of regenerative braking are to apply a negative braking torque and recovering kinetic energy in a method that enables re-use at a later time. Different methods can be used to accomplish this, either by mechanical means (flywheel, spring) or with different forms of electrical implementations (separate generator, diode rectification & supercapacitors).

With BLDC motors, the systems required for propulsion already enable a potential method for regenerative braking. The six-switch inverter and the coordination of three-phase current to control the motor to a desired speed can be modified with a unique switching strategy to support braking and regeneration. The intent of a modified switching strategy is to capitalize on the unavoidable back-emf generation while translating it into charge capable voltage & current [6].

For the control system developed, regenerative braking will be implemented using a single-switch PWM strategy. For this strategy, the existing six-switch control for the three-phase inverter will be modified such that the low-side switches (S2, S4, S6) are operating with a PWM control signal while they are expected to be operational [7]. This is detailed in Figure 2 below.

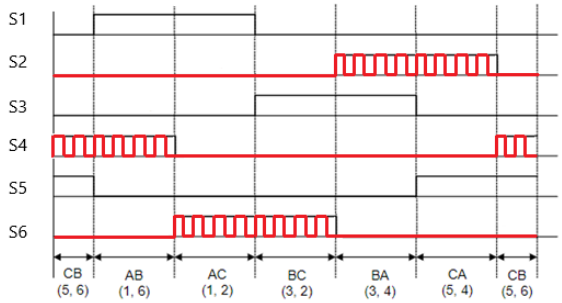

Figure 2: Single-switch PWM implementation

This control strategy introduces a method for half-wave rectification at the inverter, applied to the three phase back-emf that is generated during standard operation.

Half-wave rectification of this form translates the zero average back-emf of each phase into a positive average voltage by eliminating the negative phase. Diodes included in the inverter will allow for current to flow in the reverse direction and charge the HV battery.

Braking torque introduced by this methods is defined by the following equation [7]:

$$Brake\ Torque = \frac{k_t(2V_{emf})}{D^2 R_b + 2R} \quad (3)$$

Where:

- k_t is the motor torque constant [8]
- $2V_{emf}$ is the motor back emf
- D is the duty cycle
- R_b is the battery load resistance
- R is the armature resistance per phase

From this equation it is clear that the braking torque is limited by the internal resistances of the motor and battery. This also indicates that there is a limit to braking capability, where there is a maximum brake torque that can be applied to the vehicle is at its highest when the duty cycle is 0%.

In the simulation completed as part of this project, considerations for braking limits and when to blend friction/regen braking components was out of scope. In reality, a fully implemented braking system must comprehend these limits in order to operate safely.

II. System Setup and Assumptions

The control system proposed in this project is designed to capitalize on the back-emf that is present while a vehicle is decelerating. To accomplish this, a method for rectifying voltage within the inverter was used along with boosting capability to bring the voltage to a charge capable level.

Rectification will be accomplished using a modified control strategy for a six-switch inverter.

Boosting will require a bi-directional DC/DC converter between the HV battery and six-switch inverter. This component will also have the added benefit of balancing the system and protecting the HV battery pack.

A. *Components*

1. HV Battery Pack

An ideal HV battery pack was used from the Simscape electrical block set. The HV battery component is modeled as a single cell capable of meeting the current and voltage requirements necessary for driving the BLDC motor.

Table 1: Default battery parameters and characterization

Parameter	Value
Nominal Voltage (Vnom)	300 V
Initial State of Charge (SOC)	70 %
Capacity (Q)	30 kWh
Internal Resistance (Ri)	0.001 Ohm
Ampere-hour Rating (AH)	100 Ah
Initial Battery Charge (AH0)	70 Ah
Voltage When Charge is AH1 (V1)	270 V
Charge When No-load Voltage is V1 (AH1)	50 Ah

State of charge (SOC) for the HV battery pack was calculated during simulation. Current measured at the HV battery was translated into a final SOC using the following equation:

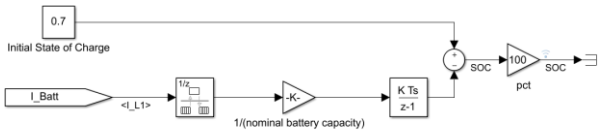

Figure 3: Simulink SOC Implementation

2. Bi-Directional DC/DC Converter

A four-switch bi-directional converter was used. This configuration was chosen due to stability and ease of control, only requiring operation in two modes. The inductor L (0.05 H) is used to limit current flow in the converter. The capacitance C (0.08 F) was included as a filtering capacitor on the inverter output side.

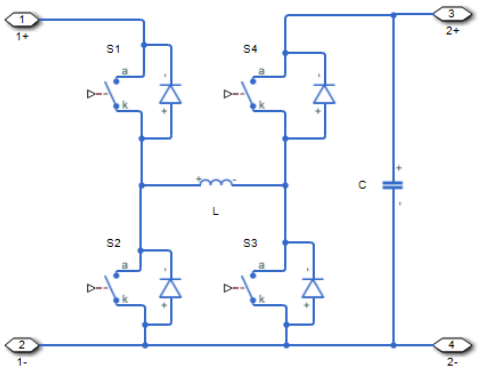

Figure 4: Bi-directional DC/DC converter configuration

When the battery voltage is greater than the inverter voltage, the converter will operate in “buck” mode. The converter sheds voltage to the inverter, charging the system. In this mode S1 is on, S2 is off, S3 and S4 are inversely controlled using the PWM control signal generated by the voltage comparison of the system.

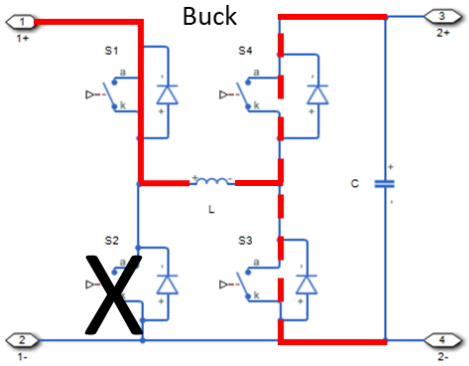

Figure 5: Bi-directional DC/DC converter in "buck" mode

When the inverter voltage is greater than the HV battery, the converter will operate in “boost” mode. In this configuration, the inverter voltage is boosted and applied to generate a charge capable voltage and current for the HV battery. In this state, S1 and S2 are inversely controlled by the same PWM control signal, S3 is off, and S4 is on.

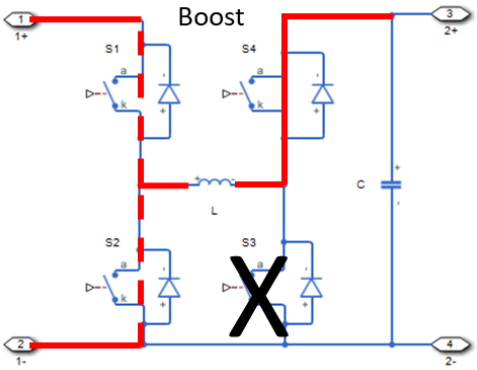

Figure 6: Bi-directional DC/DC converter in "boost" mode

The PWM control signal is determined using error between the input and output voltages and a PI controller (P=0.008, I=0.001). The mode determination is covered by comparing the input and output voltages, and the switch commutation is changed to match the mode of operation.

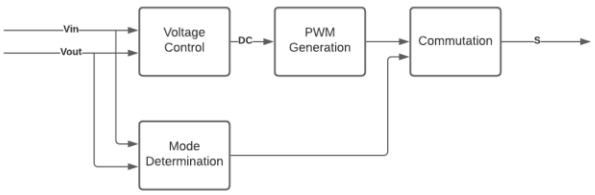

Figure 7: Bi-directional DC/DC converter control logic

3. Six-Switch Inverter

A six-switch inverter was used to translate the DC bus voltage into usable three-phase voltage for the BLDC motor. This includes the use of ideal switches and diodes.

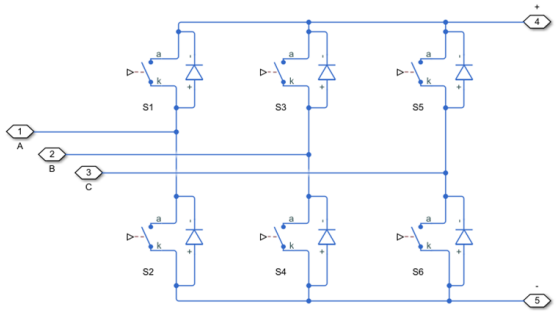

Figure 8: Six-switch inverter configuration

The six-switch inverter is controlled using the following logic:

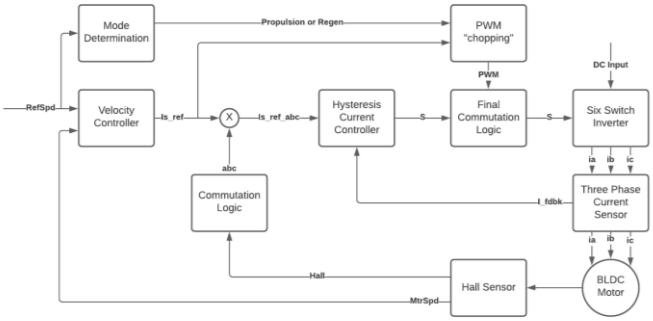

Figure 9: Six-switch inverter control logic

A hall sensor was used to determine the rotor position using back-emf measurements, mapping that to six unique intervals for switching control [8]. The velocity controller compares reference speed and motor speed feedback with a PI controller (P=7, I=0.5). The combination of the hall sensor and three phase current feedback was the input for the hysteresis current controller. With these components, the commutation logic detailed in Table 2 and Table 3.

Table 2: Interpretation of hall sensor values for motor phases

Interval	Hall Sensors			Motor Phases		
	H1	H2	H3	Phase A	Phase B	Phase C
I	1	1	0	Off	On (+)	On (-)
II	0	1	0	On (-)	On (+)	Off
III	0	1	1	On (-)	Off	On (+)
IV	0	0	1	Off	On (-)	On (+)
V	1	0	1	On (+)	On (-)	Off
VI	1	0	0	On (+)	Off	On (-)

Table 3: Switch states

Interval	Switch States					
	S1	S2	S3	S4	S5	S6
I (BC)	0	0	0	1	1	0
II (BA)	1	0	0	1	0	0
III (CA)	1	0	0	0	0	1
IV (CB)	0	0	1	0	0	1
V (AB)	0	1	1	0	0	0
VI (AC)	0	1	0	0	1	0

In addition to the standard BLDC commutation, there was a logic component included to facilitate the single switch regenerative braking strategy detailed in section I.C above. This logic component is responsible for enabling regeneration under braking. While the motor speed is decreasing it can be assumed that regeneration is being requested. If this is true, then the additional PWM control signal is applied to the low-side switches (S2, S4, S6). This added PWM will enable a controlled half-wave rectification at the inverter. While rectification is active, the diodes enable a current path which in turn allows the bi-directional DC/DC converter to charge the HV battery.

4. BLDC Motor Model

An ideal BLDC motor was used from the Simscape electrical block set. Parameters were chosen to match real-world characteristics of a 100kW motor. These parameters are listed in Table 4 below.

Table 4: BLDC Motor Parameterization

Parameter	Value
Rotor Angle for Constant Back EMF	$\pi/14$ rad
Maximum Rotor-Induced Back EMF	400 V
Rotor Speed Used for Back EMF measurement	2000 rpm
Number of Pole Pairs	4
Stator Self-Inductance Per Phase (Ls)	0.2 mH
Stator Inductance Fluctuation (Lm)	0 H
Stator Resistance Per Phase (Rs)	0.013 Ω
Rotor Inertia	1 kg/m^2
Rotor Damping	0.2 Nms

The motor itself is connected to a highly simplified driveline consisting of an inertial load and the hall sensors. For the purpose of this model and analysis any additional road, wind, or friction losses associated with vehicle dynamics will be neglected.

5. Driver Model

The six-switch control system required a reference motor speed input. Drive cycles were run using desired vehicle speed in kph, with calculations to determine the correlated motor speed. These calculations assumed a 44 cm tire with a 7-times gear reduction to the motor itself – matching a drivetrain and vehicle design similar to that of a Chevrolet Bolt EV.

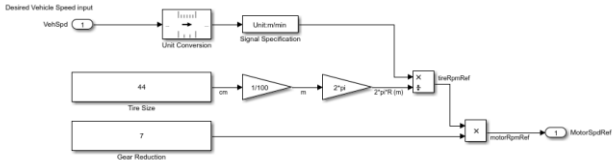

Figure 10: Simulink motor reference speed calculation

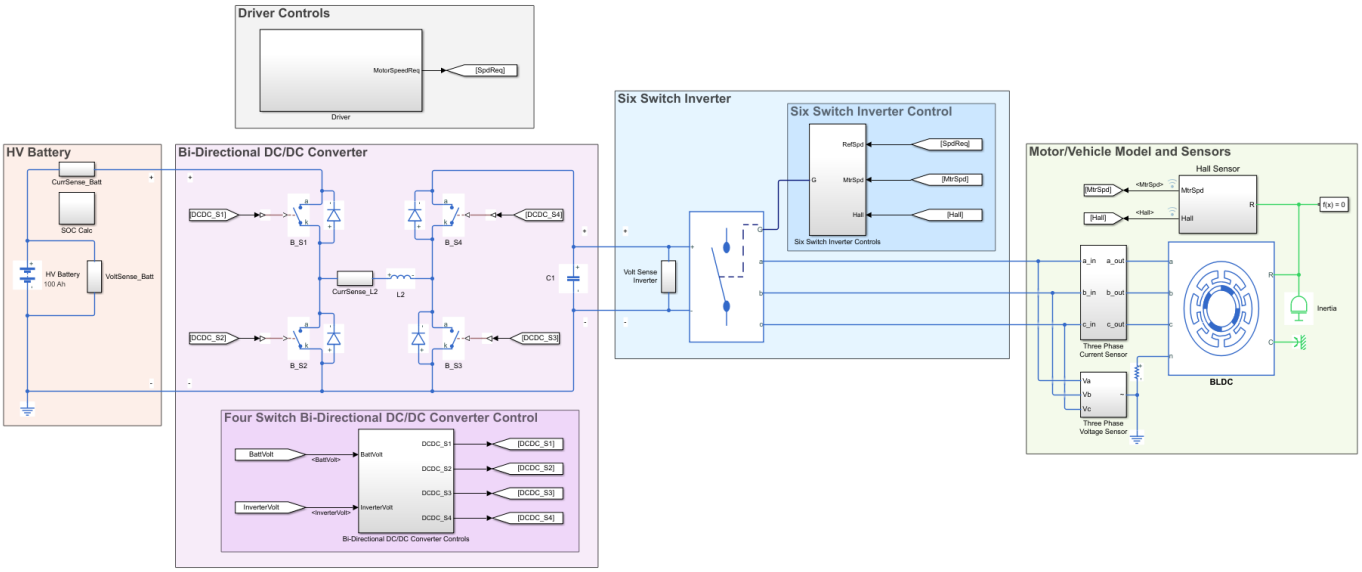

Figure 11: Simulink model with all system components

III. Simulation & Results

A. System Performance

A ramp & hold drive cycle was used to detail the standard operation of the system. In this cycle the vehicle speed gradually increases to 20 kph, holds at speed, then gradually decreases to 0 kph.

The system is capable of following the vehicle speed allowing for limited error over time.

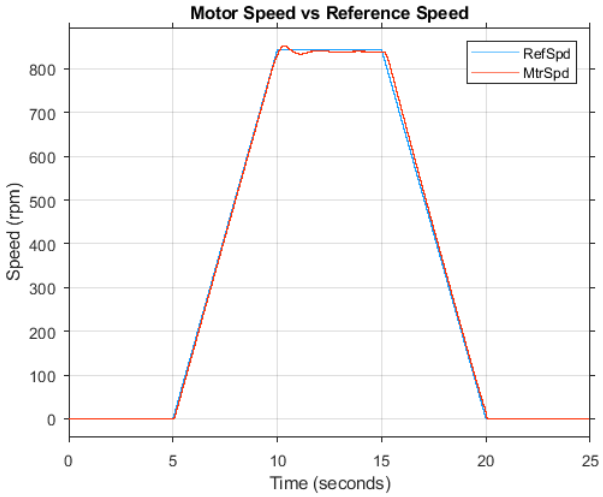

Figure 12: Motor speed vs. reference speed

It is important to note that the introduction of low-side PWM for regeneration when the motor speed is decelerating does not have any significant impact on the motor speed error.

The system as designed is capable of fully reducing vehicle speed by regenerative braking. There is no friction brake component modeled. As such, the simulation will only be valid for maneuvers that are within the brake torque capability. This is a limit of the system model itself, and one area that can be highlighted for future improvement.

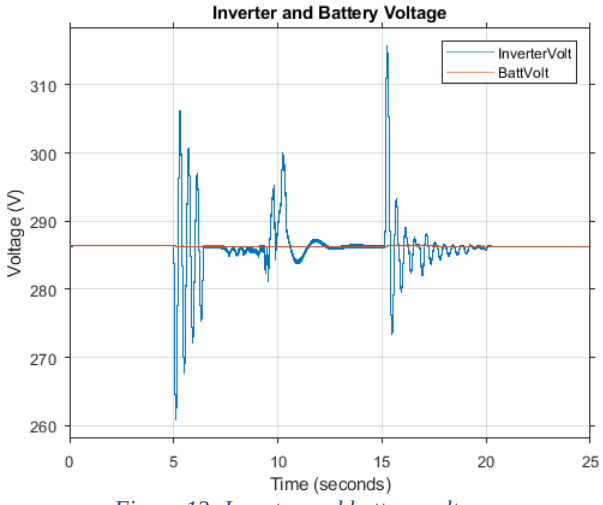

Figure 13: Inverter and battery voltage

The inverter and battery voltages are balanced by the bi-directional DC/DC converter for the majority of the drive cycle. Significant voltage oscillations at the inverter can be seen when there are large jumps in acceleration for the system.

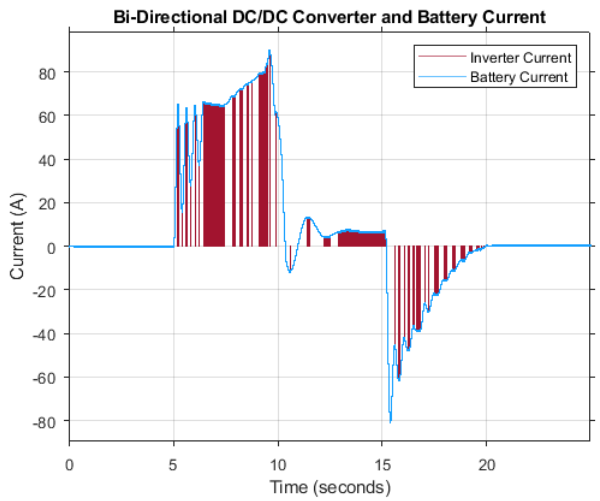

Figure 14: Bi-directional DC/DC converter and battery current

Current is the driving factor for charging or discharging the HV battery. If current at the battery is positive, it will be discharging. If current at the battery is negative, it will be charging. Current measurements in Figure 14 match the expected performance for the ramp drive cycle.

The addition of the low-side PWM switch control for regeneration enables the current to stay completely negative for the entirely of the deceleration portion of the drive cycle.

Current measured at the bi-directional DC/DC converter details the impact of the buck/boost modes. In the buck mode, the inverter current PWM will oscillate between 0 A and the battery current waveform as the switches toggle based on the PWM control signal.

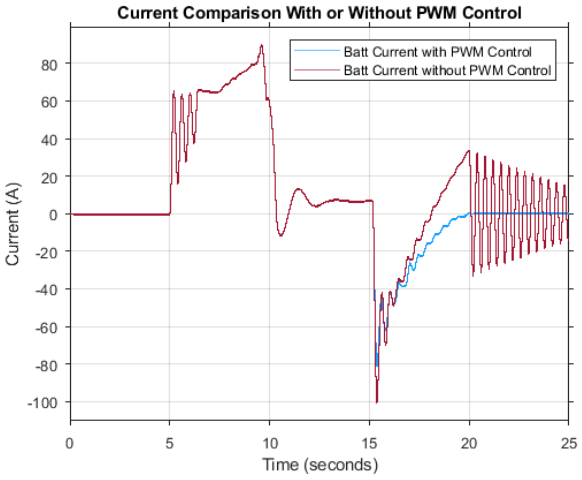

Figure 15: Current comparison with or without PWM control

Considering the current measurements at the HV battery, the PWM control feature has the most impact on keeping the current negative throughout the entirety of the deceleration portion of the drive cycle. Figure 15 above details the difference. To maintain the deceleration and proper braking torque without adding a frictional brake component, the BLDC motor needs to increase the current draw. When the battery is providing current to maintain the decelerating motor (positive current measured at battery), it is no longer regenerating. This is the main benefit of the low-side PWM control, where the rectification will ensure that current is only being added to the HV battery during deceleration.

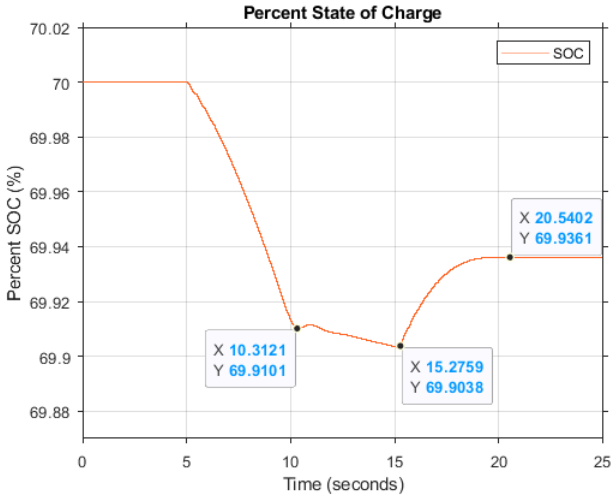

Figure 16: Percent state of charge

The measured state of charge details the impact of each section for the drive cycle. Initial acceleration up to the desired vehicle speed requires the most amount of energy, while holding the vehicle speed constant consumes a significantly less amount of energy.

Energy consumed from the discharge portion of the drive cycle was calculated to be 96.2 mAh.
Energy recovered in the recharge portion of the drive cycle was calculated to be 32.3 mAh.

For this drive cycle and system configuration, 34.2% of the energy consumed for propulsion was recovered on braking

B. PWM Variation Analysis

As listed in equation (3) above, the duty cycle of the PWM applied to each of the low-side switches will impact the braking torque generation. In addition, the duty cycle will also change the effectiveness of energy recovery in a similar manner.

An analysis was completed where the duty cycle applied was varied from the 100-20% and compared with the PWM control signal implementation. With a duty cycle of 100%, the feature to apply any PWM on the switching signal is nullified. Operation at this duty cycle is exactly what would be seen in normal hysteresis control without a modified switching strategy. Final SOC measured after completing the deceleration cycle was compared between the different strategies.

Figure 17 below details the result of this analysis:

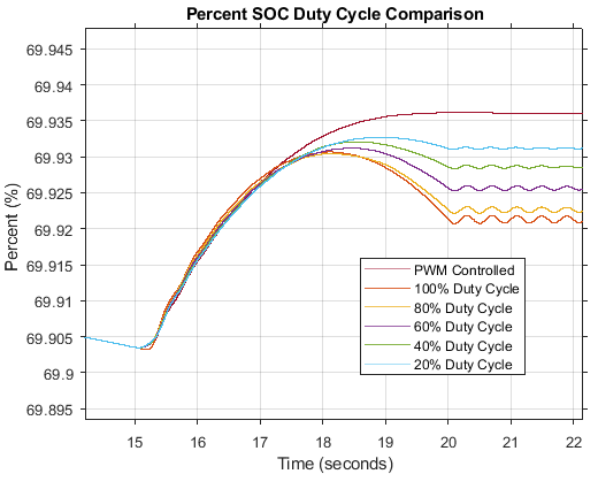

Figure 17: Percent SOC duty cycle comparison

As expected, the implementation of a PWM controlled signal was the most effective method of regeneration. Details on the energy recovered for each value analyzed is listed in Table 5 below.

Table 5: PWM variation energy recovery values

Duty Cycle	Energy Recovered
100 %	17.2 mAh
80 %	19.2 mAh
60 %	22.2 mAh
40 %	24.2 mAh
20 %	28.2 mAh
PI Controlled	32.3 mAh

With a 100% duty cycle there is a minimal level of regeneration before the system ultimately has to consume energy once again to keep the motor speed in the desired range.

As the duty cycle decreases, the point with which the system must switch from fully regenerating to requiring energy consumption is further into the deceleration profile. With this, it is clear that a low duty cycle – matching a high level of inverter rectification – will be ideal for enabling full braking capability.

C. *Three Phase Current and Voltage*

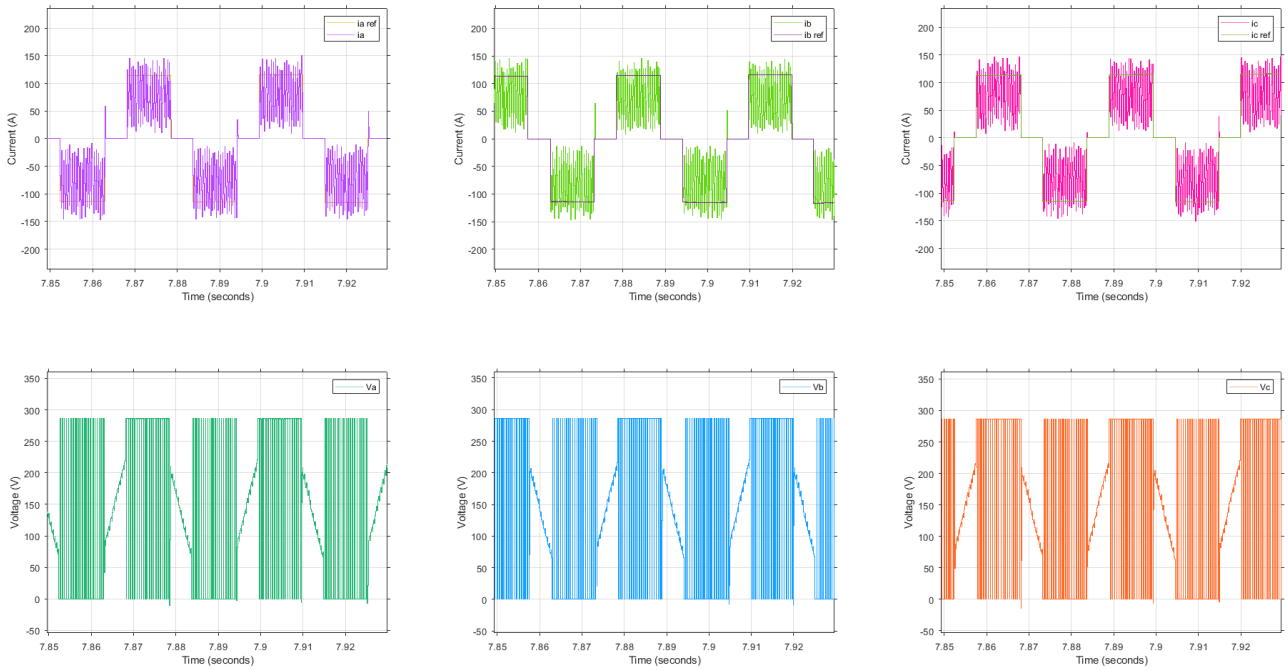

Figure 18: Three phase current and voltage during propulsion

Three phase current and voltage were measured at the inverter. Figure 18 above shows waveforms under propulsion – matching the expected trapezoidal form. Figure 19 below shows the same waveform under regeneration. The additional half-wave rectification changes the current and voltage profiles as the back-emf is translated into a charge capable voltage. Included as part of the three-phase current reference is the square control-wave for hysteresis control. This details how the hysteresis control of the six-switch inverter can translate into the three-phase current output that drives the BLDC motor.

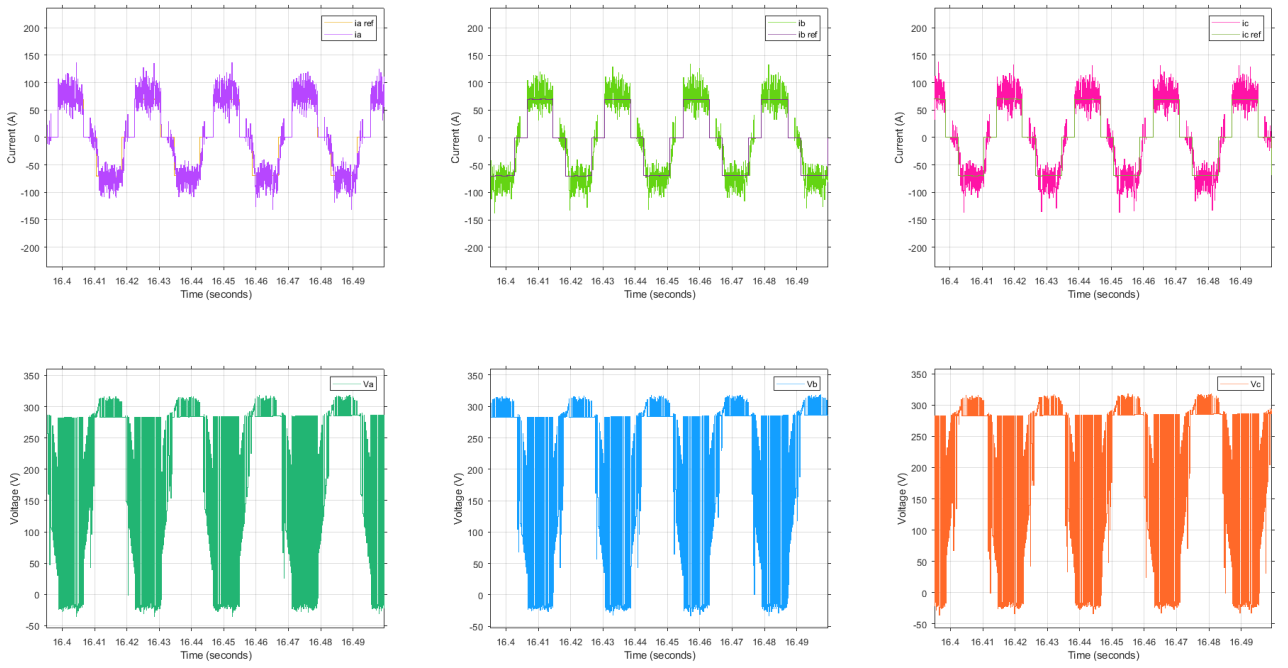

Figure 19: Three phase current and voltage during regeneration

IV. Conclusion

Regenerative braking enables greater levels of energy efficiency for hybrid and battery electric vehicles. This project details only one of many different control strategies that have been used with BLDC motors for regenerative braking. The implementation details the fundamentals of the process and builds a framework for testing and validation.

There are several improvements to this project that could be completed as future work. Model fidelity can be improved to enable more accurate simulation data – specifically regarding the HV battery and vehicle dynamics. It would also be desirable to move away from ideal switches and diodes for the six-switch inverter and bi-directional DC/DC converter. Additional control strategies could also be implemented, comparing the regenerative capability as well as the impact on braking torque.

V. References

[1] D. Torres and P. Heath, "Regenerative Braking of BLDC Motors," [Online]. Available: http://ww1.microchip.com/downloads/en/devicedoc/regenerative%20braking%20of%20bldc%20motors.pdf. [Accessed 5 December 2021].

[2] Wikipedia contributors, "Brushless DC electric motor," Wikipedia, 3 December 2021. [Online]. Available: https://en.wikipedia.org/w/index.php?title=Brushless_DC_electric_motor&oldid=1058375413. [Accessed 11 December 2021].

[3] Toshiba Electronic Devices & Storage Corporation, "120° Square-Wave Commutation," 03 August 2018. [Online]. Available: https://toshiba.semicon-storage.com/info/docget.jsp?did=61176. [Accessed 5 December 2021].

[4] H. Sevian, "Faraday's Law," Boston University, 18 February 1998. [Online]. Available: http://buphy.bu.edu/py106/notes/FaradaysLaw.html. [Accessed 5 December 2021].

[5] MathWorks, "Three-winding brushless DC motor with trapezoidal flux distribution," MathWorks, 2021. [Online]. Available: https://www.mathworks.com/help/physmod/sps/ref/bldc.html?searchHighlight=BLDC&s_tid=srchtitle_BLDC_1. [Accessed 5 December 2021].

[6] N. Z. A. B. P. Tawadros, "17 - Integration and performance of regenerative braking and energy recovery technologies in vehicles," *Alternative Fuels and Advanced Vehicle Technologies for Improved Environmental Performance*, pp. 541-563, 2014.

[7] V. S. A. Joseph Godfrey, "A new electric braking system with energy regeneration for a BLDC motor driven electric vehicle," *Engineering Science and Technology, an International Journal*, vol. 21, no. 4, pp. 704-713, 2018.

[8] D. Collins, "FAQ: What is trapezoidal back EMF?," Motion Control Tips, 28 April 2016. [Online]. Available: https://www.motioncontroltips.com/faq-trapezoidal-back-emf/. [Accessed 5 December 2021].

[9] J. K. Jr, "6.061 Class Notes, Chapter 12: Permanent Magnet "Brushless DC" Motors," 2011. [Online]. Available: https://ocw.mit.edu/courses/electrical-engineering-and-computer-science/6-061-introduction-to-electric-power-systems-spring-2011/readings/MIT6_061S11_ch12.pdf. [Accessed 6 December 2021].

[10] WEG Motors, "Specification of Electric Motors," 1 March 2020. [Online]. Available: https://static.weg.net/medias/downloadcenter/ha0/h5f/WEG-motors-specification-of-electric-motors-50039409-brochure-english-web.pdf. [Accessed 6 December 2021].